5.1.6 Effect of Physical Properties

Physical properties of the liquids affect gas holdup. In this project, the viscosity of the liquids used varied from 1 to 19 cP, the surface tension from 32 to 72 dynes/cm and the density from to 0.97 to 1.17 g/mL (see Table 8). Because more than one property was varied at any given time, the effect of physical properties cannot be completely analyzed. However, based on our data and published data, a few qualitative conclusions can be drawn.

Both liquid viscosity and surface tension affect gas holdup. A decrease in either seems to increase gas holdup. Comparing our results with water and tetralin (Figures 12 and 13), one can see that gas holdup was larger when tetralin was used. The surface tension of tetralin is 32 dynes/cm, compared to 72 dynes/cm for water but tetralin has a higher viscosity (2.65 vs. 1 cP). Even though these are opposite effects, the increased holdup indicates that surface tension may have a greater effect than viscosity. Hikita and Kikukawa's correlation confirms this conclusion.

Experiments with glycol/water mixtures show that both viscosity and surface tension affect gas holdup: decreasing the glycol content from 100 to 50 wt % increased gas holdup. At the same time, both viscosity and surface tension were changed. Due to the significant drop in viscosity from 19.00 to 4.1 cP gas holdup should have increased although the surface tension was increased slightly from 48.2 to 56.7 dynes/cm.

Although density was varied only slightly, it also appeared to affect gas holdup. This effect is obvious when comparing results with tetralin and 50 wt % glycol systems. Both the viscosity and surface tension of tetralin are lower than those of the 50 wt % glycol/water mixture. Hence one would expect tetralin to exhibit a higher gas holdup. However, the differences in holdup values for the two systems are negligible. Tetralin had a lower density than the 50 wt % glycol/water mixture, indicating that liquid density also may play an important role.

Table 8

Physical Properties of Different Liquid Systems

Liquid system	Temp.(°C)	Density (g/ml)	Viscosity,(cP)	Surface tension (dynes/cm)
100% glycol	25	1.17	19.00	48.2
90 wt. glycol	21.6	1.107	13.08	45.9
70 wt. glycol	21.6	1.091	6.40	48.8
50 wt. glycol	18.5	1.078	4.10	56.7
Tetralin		0.97	2.65	32
Water		1	1	72

Our results show that physical properties do affect the gas-holdup values. However, because our experiments were limited, a detailed discussion of the effect of every macroscopic physical property is not feasible. In addition, one should point out that foaming characteristics of these liquids also play an important part in determining gas holdup. Unfortunately, just by knowing the values of the density, surface tension, and viscosity, one cannot predict the foaming characteristics. At this point, a rational approach is to predict gas-holdup values for the demonstration plant dissolver with reasonable accuracy.

5.1.7 Correlations

Several correlations for determining gas holdup in bubble columns have been published. Recently, Irwin et al., (50) examined several correlations in order to determine the most suitable for modelling coal-liquefaction dissolvers. Correlations were within ± 20% of each other, indicating that more than one correlation can be successfully used to predict gas holdup. Because several correlations can be used successfully, developing a new correlation is not really necessary; in addition, the limited amount of data available from this program is not sufficient to develop a good correlation. Hence, in this section, we attempt to identify the correlation(s) that can be used to predict our experimental data.

Table 9 lists the correlations that were used to predict gas holdup in bubble columns. These correlations show that different investigators found that physical properties of the fluid systems affect gas holdup differently. In general, most observers found that gas holdup can be simply expressed by:

$$\varepsilon_g \propto V_g^{\,n}$$

where V_g is the superficial gas velocity. The values of the exponent vary widely in this investigation between 0.52 and 0.79 for the systems that were studied. Very few correlations consider the gas

Table 9

Correlations for Predicting Gas Holdup

Akita and Yoshida (26)

$$\frac{\varepsilon_g}{(1-\varepsilon_g)^4} = C_1 (N_{Bo})^{1/8} (N_{Ga})^{1/2} (N_{Fr})$$

Hikita and Kikukawa (3)

$$\varepsilon_g = 0.505\ V_G^{0.47} \left(\frac{72}{\sigma}\right)^{2/3} \left(\frac{1}{\mu}\right)^{0.05}$$

Hughmark (16)

$$\varepsilon_g = \frac{V_{sG}}{U_s} \left[\left(\frac{62.4}{\rho_L}\right) \quad \left(\frac{72}{\sigma}\right)\right]^{1/3}$$

Pilhofer et al. (51)

$$\frac{\varepsilon_g}{1-\varepsilon_g} = 0.115[V_g^3/(\upsilon g \Delta\rho/\rho_L)]^{0.23}$$

ε_g = gas holdup
V_g = superficial gas velocity (ft/sec)
U_s = slip velocity (ft/sec)
ρ_L = liquid density (lb/ft^3)
σ = dynes/cm
D = diameter of column (ft)
C_1 = 0.20 for nonelectrolytes
0.25 for electrolytes

υ = kinematic viscosity (ft^2/sec)
g = gravitational acceleration
32.2 (ft/sec^2)
μ = liquid viscosity (cp)
N_{Bo} = $gD^2\rho_L/\sigma$ (Bond number)
N_{Ga} = gD^3/υ_L^2 (Galileo number)
N_{Fr} = $V_g/\sqrt{gD}$ (Froude number)

properties. However, for the system we studied, gas properties were similar because nitrogen and air were used. Most investigators agree that surface tension dramatically affects gas holdup, even though the magnitude of the effect varies. Pilhofer et al. (51) did not include the effect of surface tension in their correlation. Several investigators related gas holdup to a ratio of the surface tension of the liquid studied and that of water. The effect of viscosity on gas holdup has also been recognized by most investigators; however, a few have ignored the effect of liquid viscosity. Also, few investigators have considered the effect of liquid density on gas holdup.

Earlier, we showed that gas holdup is affected by both surface tension and viscosity. Hence a single correlation that could fit all our data should include both viscosity and surface tension. Akita and Yoshida's correlation (12) fits in this mold. A few other correlations were also investigated. Akita and Yoshida's correlation predicted the results from air/water reasonably well, but underpredicted our results for tetralin and glycol/water mixtures. For tetralin, correlations of Pilhofer et al. (15) and Hughmark (16), predict the data reasonably well (Figure 34). Hughmarks's correlation does not predict the glycol/water very well, possibly because viscosity is not considered.

Pilhofer's correlation does not reasonably predict gas holdup for the glycol/water mixture at concentrations we studied; for pure glycol it does provide a reasonable fit with the data. Akita and Yoshida's correlation has a proportionality constant; the value recommended for this constant (C_1) is 0.20 for nonelectrolytes and 0.25 for electrolytes. If one considers ethylene glycol as a weak electrolyte, then the use of 0.25 for the constant results in good predictions for the gas-holdup values. Tetralin is not an electrolyte. However, the use of 0.25 for C_1 in the case of tetralin also results in a reasonably good agreement with experimental data.

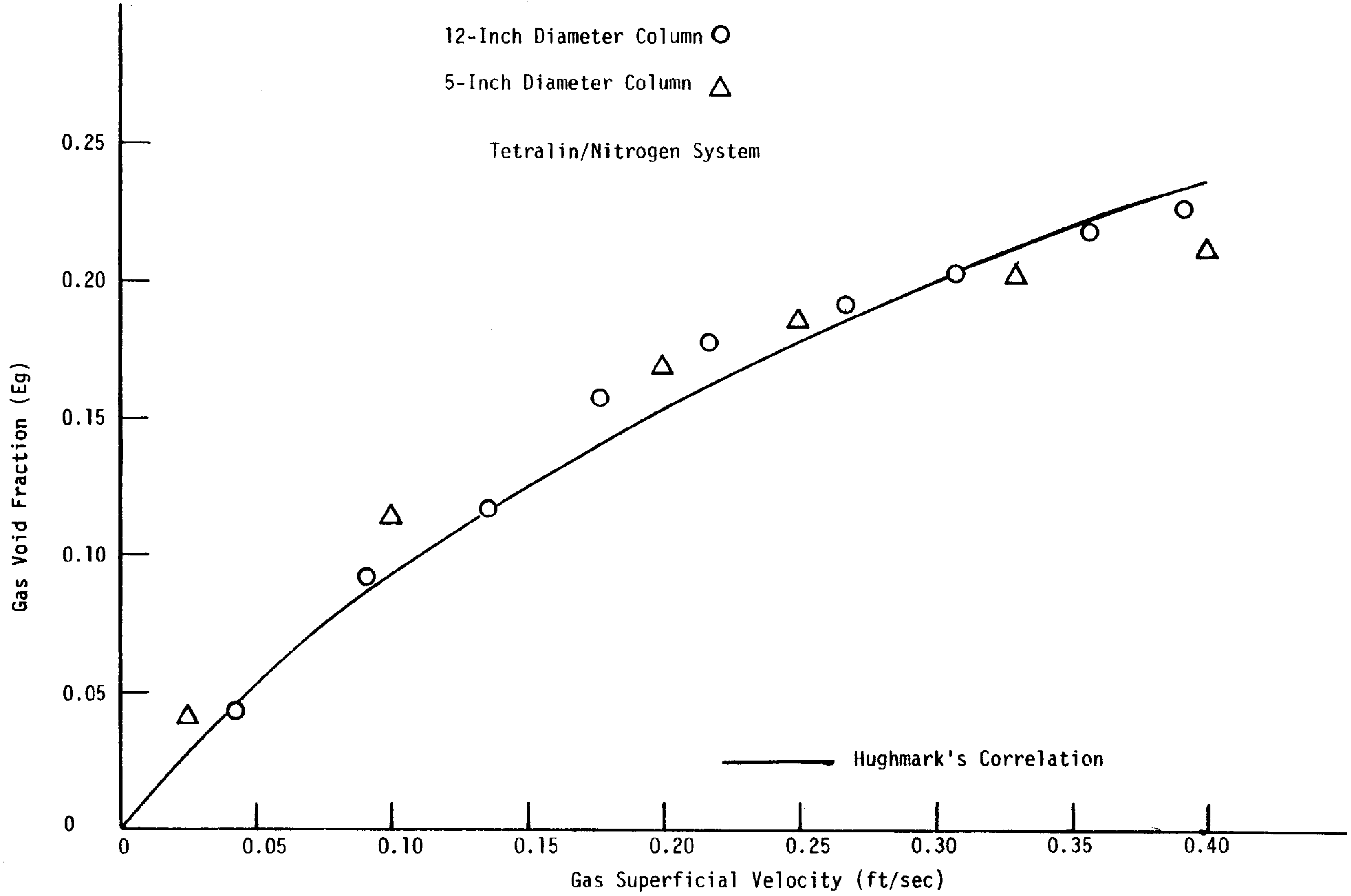

Figure 34

Comparison of Hughmark's Correlation with Experimental Data

One can conclude that a single correlation is not effective in predicting our experimental gas-holdup values. Akita and Yoshida's correlation is quite reasonable except for the tetralin data, but with minor corrections, it can be used effectively.

5.2 Liquid Dispersion

The axial liquid dispersion coefficient (E_{zL}) is an important quantity that is needed to describe the hydrodynamics taking place in the dissolver. Its magnitude indicates how much turbulent exchange takes place axially in the column. Usually, the assumption is made that radial liquid dispersion is much higher than axial. Hence, uniformity of liquid velocity and dye concentration in the radial direction can be assumed.

Most of the experiments conducted for axial liquid dispersion were in the 12-in. column, although two runs with the tetralin were conducted in the 5-in. column. We used two methods to measure the axial dispersion number: batch (no liquid flowing) and continuous (liquid flow).

5.2.1 Theoretical Background

5.2.1.1 Batch Model

A basic one dimensional diffusion model was applied to our data. We used an equation from Ohki et al. (5):

$$\frac{\partial c}{\partial t} = E_{zL} \frac{\partial^2 c}{\partial z^2} \qquad (1)$$

where c = tracer concentration, z = axial distance (ft), and E_{zL} = liquid axial dispersion coefficient (ft^2/sec).

Assuming an impulse injection, the approximate solution is obtained with equation 2.

$$C' = 1 + 2 \sum_{n=1}^{\infty} \left[\left(\cos \frac{\pi n}{L} Z\right)\exp\left(-n^2 \frac{\pi^2}{L^2} E_{zL} t\right)\right] \qquad (2)$$

where C' = nondimensional tracer concentration and L = total length of aerated liquid.

This approximate solution is within 1% of the complete analytical solution. Equation 2 was used to obtain the value of E_{zL}. Hence by obtaining Z/L at a particular sampling site and determinig C' as a function of t from the experiment, one can calculate E_{zL}. Ideally, one point on the curve of C' and t should be sufficient to determine E_{zL}. In actuality, three points were selected in the range of C' between 0.3 and 0.8, from which three values of E_{zL} were calculated. The average E_{zL} value was then reported for that particular gas velocity. A separate method was used to determine E_{zL} and to compare with the average value obtained from the technique described above. This method involves at least-square fits program to optimize the value of E_{zL} to best fit the entire tracer curve. A comparison of these two methods will be discussed later.

5.2.1.2 Continuous Model

The basic one-dimensional model used for the continuous-flow experiments is:

$$\frac{\partial c}{\partial t} + \frac{\partial c}{\partial z} = \frac{E_{zL}}{uL} \frac{\partial^2 c}{\partial z^2} \qquad (3)$$

where c = non-dimensional tracer concentration; t = non-dimensional time from injection; z = non-dimensional axial distance; E_{zL} = axial liquid dispersion coefficient (ft^2/sec); L = length of dispersion vessel considered (ft); u = liquid flow velocity (ft/sec); $E_{zL}/uL = 1/Pe$; and Pe = Peclet number. Boundary conditions used for this model are for closed vessel. The model was solved numerically.

5.2.2 Air/Water and Air/Water/Sand Systems

Liquid dispersion experiments were performed in the 12-in. diameter column for both two- and three-phase systems. The ranges of variables investigated are summarized in Table 10. Fits of all the experimental tracer curves with theoretical curves from the axial dispersion model are displayed in Appendices A and C. In these curves, circles represent the experimental tracer curve and the solid line represents the theoretical predicted curve.

Matching experimental and theoretical curves was found to be sensitive to column height. Because the dispersion number (E_{ZL}/uL, a dimensionless quantity) is inversely proportional to the height of the column, determination of the dispersion number by the best-fit technique became more difficult with increasing column height. The curve-matching technique was extremely sensitive to any tailing in the curve. Since some fits were less perfect than others because of tailing problems, a consistent method of selecting the dispersion numbers was developed. Dispersion numbers were always determined by fitting the peak time (peak position) of the tracer curve with the dispersion model, because peak time was not affected by tailing in the experimental curve. Tailing only changed the height of the curve. As long as the mean residence time could be measured accurately, peak position was the best way to match dispersion numbers.

Fluctuations in liquid flow could cause errors in the determination of mean residence time if averages of several discrete measurements were used. In addition, mean residence times, which were calculated using the experimental tracer curve, were compared with the values calculated using average flow rates. Whenever a large (greater than 10%) discrepancy existed between the two numbers, the residence time calculated using the experiment tracer curve was used to generate the tracer curves. This procedure also improved data analysis.

Table 10

Liquid Dispersion: Two- and Three-Phase Flow

Variable Studies

Liquid velocity	0.01-0.07 ft/sec
Gas velocity	0.0-0.43 ft/sec
Particle size	20/30 mesh, 60/80 mesh, -100 mesh, and -140 mesh
Solids Concentration	2-20 lb/ft^3
Distributor	No distributor, distributors #1 and #2

Incorporating all these improvements, a new method was tried to determine the liquid dispersion coefficients for experiments using distributor No. 2. Based on the theoretical curves for the axial dispersion model, a curve showing the relationship between peak time and peclet number was developed. This curve is shown in Appendix B. Knowing the peak time from the experimental data, the Peclet number can be determined using the above curve. This method is less time consuming than trying to match the experimental and theoretical curves. In order to check the precision of the method, a few liquid dispersion coefficients were determined by using both methods; namely, by matching the experimental and theoretical curves and by using the peak time vs. peclet number curve. The comparison is shown in Table B-1 (Appendix B). As can be seen from the table, this method is equally good as the method comparing theoretical and experimental curves. Since this method is less time consuming, this method was used to determine the liquid dispersion coefficients for experiments using distributor No. 2.

The liquid dispersion coefficients and their operating conditions are tabulated in Table 11. The axial dispersion coefficients were not reported for those experiments in the absence of gas flow. The tracer curves in the absence of gas flow approached plug-flow regime: the curves rose steeply and the peak times were very close to a dimensionless time of unity. However, tailing problems existed in the experimental tracer curves and could not be handled by the axial dispersion model.

As discussed in the Experimental Section, a constant solid concentration should be maintained in the column in order to determine the effects of solids on liquid dispersion. For practical purposes, slurry was not pumped into the column. Instead, a predetermined amount of sand was added to the column partially filled with liquid. Then the liquid dispersion experiments proceeded with the liquid flowing through the column at various rates. For large particles (20/30 mesh and 60/80 mesh), only slight amounts of solid were lost as entrained particles in the existing stream. However, for very fine particles

Table 11
Liquid Dispersion Experimental Results

Run no.	Liquid velocity (ft/sec)	Gas velocity (ft/sec)	Particle size (mesh)	Solids concentration (lb/ft^3)	dispersion^a no.	Axial dispersion coefficients (ft^2/sec)
			Distributor #1			
XIII - 1	0.0489	0.327	--	0.0	0.50	0.617
- 2	0.0505	0.194	--	0.0	0.39	0.497
- 3	0.0410	0.194	--	0.0	0.47	0.486
- 4	0.0302	0.194	--	0.0	0.65	0.495
- 5	0.0199	0.194	--	0.0	1.00	0.502
- 6	0.0099	0.194	--	0.0	2.00	0.500
- 7	0.0506	0.097	--	0.0	0.38	0.485
- 8	0.0499	0.050	--	0.0	0.32	0.403
- 9	0.0048	0.050	--	0.0	3.2	0.406
- 10	0.0503	0.0	--	0.0	Very low	Very low
- 11	0.0097	0.327	--	0.0	2.5	0.612
- 12	0.0190	0.327	20/30	5.0	1.00	0.479
- 13	0.0400	0.327	20/30	5.0	0.47	0.474
- 14	0.0598	0.327	20/30	5.0	0.32	0.482
- 15	0.0092	0.327	20/30	5.0	2.20	0.511
- 16	0.0295	0.327	20/30	5.0	0.65	0.483
XIV - 1	0.0536	0.050	20/30	5.0	0.22	0.297
- 2	0.0541	0.097	20/30	5.0	0.25	0.341
- 3	0.0535	0.194	20/30	5.0	0.27	0.364
- 4	0.0533	0.327	20/30	5.0	0.35	0.471
- 5	0.0534	0.0	20/30	5.0	Very low	Very low
XV - 1	0.0548	0.50	20/30	20.0	0.22	0.304
- 2	0.0532	0.097	20/30	20.0	0.22	0.295
- 3	0.0538	0.194	20/30	20.0	0.27	0.366
- 4	0.0497	0.327	20/30	20.0	0.30	0.376
- 5	0.0537	0.0	20/30	20.0	Very low	Very low
- 6	0.0404	0.327	20/30	20.0	0.35	0.356
- 7	0.0285	0.327	20/30	20.0	0.70	0.503
- 8	0.0255	0.327	20/30	20.0	0.60	0.385
- 9	0.0130	0.327	20/30	20.0	0.60	0.196

Table 11 (Continued)

Run no.	Liquid velocity (ft/sec)	Gas velocity (ft/sec)	Particle size (Mesh)	Solids concentration (lb/ft^3)	dispersion[a] no.	Axial dispersion coefficients (ft^2/sec)
XVI - 1	0.016	0.080	-140	2.06 to 19.33	0.9	0.33 to 0.38
- 2	0.043	0.327	100	4.88 to 9.47	0.5	0.53 to 0.55
XVII - 1	0.017	0.327	60/80	5.0	1.00	0.43
- 2	0.031	0.327	60/80	5.0	0.5	0.38
- 3	0.049	0.0	60/80	5.0	Very low	Very low
- 4	0.035	0.327	60/80	5.0	0.5	0.44
- 5	0.055	0.5	60/80	5.0	0.22	0.30
- 6	0.069	0.097	60/80	5.0	0.20	0.35
- 7	0.050	0.327	60/80	5.0	0.33	0.42
- 8	0.057	0.194	60/80	5.0	0.27	0.38
- 9	0.954	0.327	60/80	5.0	0.35	0.48
XVIII - 1	0.045	0.050	60/80	20.0	0.20	0.23
- 2	0.050	0.194	60/80	20.0	0.27	0.34
- 3	0.041	0.327	60/80	20.0	0.43	0.45
- 4	0.018	0.327	60/80	20.0	1.0	0.46
(b)XIX - 1	0.049	0.327	-140	5.0	0.35	0.43
			Distributor #2			
XXV - 1	0.053	0.05	--	--	0.27	0.361
- 2	0.048	0.10	--	--	0.35	0.424
- 3	0.052	0.194	--	--	0.37	0.485
- 4	0.050	0.33	--	--	0.38	0.479
- 5	0.058	0.43	--	--	0.42	0.615
- 6	0.048	0.0	--	--	Very low	Very low
- 7	0.036	0.33	--	--	0.67	0.609
- 8	0.021	0.33	--	--	1.02	0.540

Table 11 (Continued)

Run no.	Liquid velocity (ft/sec)	Gas velocity (ft/sec)	Particle size (mesh)	Solids concentration (lb/ft^3)	dispersion no.[a]	Axial dispersion coefficients (ft^2/sec)
XXVI - 1	0.056	0.05	20/30	5.0	0.17	0.240
- 2	0.053	0.10	20/30	5.0	0.30	0.401
- 3	0.051	0.194	20/30	5.0	0.30	0.386
- 4	0.050	0.33	20/30	5.0	0.32	0.403
- 5	0.034	0.43	20/30	5.0	0.65	0.558
- 6	0.038	0.33	20/30	5.0	0.45	0.431
- 7	0.020	0.33	20/30	5.0	0.85	0.429
- 8	0.048	0.05	20/30	20.0	0.19	0.230
- 9	0.048	0.10	20/30	20.0	0.20	0.242
- 10	0.048	0.194	20/30	20.0	0.27	0.327
- 11	0.048	0.33	20/30	20.0	0.30	0.363
- 12	0.048	0.43	20/30	20.0	0.35	0.424
- 13	0.037	0.33	20/30	20.0	0.345	0.322
- 14	0.021	0.33	20/30	20.0	0.70	0.371
XXV11 - 1[b]	0.049	0.03	-140	3.74	0.33	0.408
XXVIII - 1[b]	0.059	0.05	-140	3.74	0.16	0.238
- 2	0.058	0.10	-140	3.74	0.25	0.366
- 3	0.050	0.194	-140	3.74	0.35	0.442
- 4	0.047	0.43	-140	3.74	0.46	0.545
- 5	0.046	0.33	-140	3.74	0.36	0.418
- 6	0.025	0.33	-140	3.74	0.72	0.454

Table 11 (Continued)

Run no.	Liquid velocity ft/sec	Gas velocity ft/sec	Particle size mesh	Solids concentration lb/ft^3	dispersion[a] no.	Axial dispersion coefficients ft^2/sec
XXIX - 1[b]	0.057	0.05	-140	14.94	0.19	0.273
- 2	0.050	0.33	-140	14.94	0.32	0.404
- 3	0.052	0.10	-140	14.94	0.33	0.433
- 4	0.051	0.194	-140	14.94	0.34	0.437
- 5	0.049	0.43	-140	14.94	0.33	0.408
- 6	0.038	0.33	-140	14.94	0.37	0.355
- 7	0.028	0.33	-140	14.94	0.48	0.39
			No Distributor			
XX - 1	0.046	0.327	--	--	0.80	0.928
- 2	0.053	0.194	--	--	0.56	0.749
- 3	0.050	0.050	--	--	0.18	0.227
- 4	0.051	0.100	--	--	0.25	0.324
- 5	0.048	0.0	--	--	Very low	--
- 6	0.041	0.327	--	--	0.50	0.513
- 7	0.015	0.327	--	--	1.30	0.475
XX1 - 1	0.049	0.194	20/30	5.0	0.38	0.472
XX1 - 1R	0.053	0.194	20/30	5.0	0.33	0.437
- 2	0.027	0.327	20/30	5.0	0.62	0.418
- 3	0.055	0.050	20/30	5.0	0.25	0.348
- 4	0.021	0.194	20/30	5.0	0.88	0.466
XX11 - 1[b]	0.053	0.194	-140	5.0	0.30	0.404
- 2	0.054	0.05	-140	5.0	0.15	0.204
X11 - 3[b]	0.024	0.327	-140	5.0	0.62	0.369
- 4	0.023	0.194	-140	5.0	0.78	0.452

---

[a] Dispersion number is the reverse of the Peclet number.

[b] Continuous operation.

(-140 mesh and -100 mesh), large amounts of sand were carried out of the column by the liquid. This resulted in an enormous difference in solid concentration between the beginning and end of the run as shown in Runs XVI-1 and XVI-2 of Table 11. Therefore, averaging extreme concentration values was not justified for very fine particles. Hence, the axial dispersion coefficients for Runs XVI-1 and XVI-2 are presented as a range rather than as a single number. Since Run XIX-1 shown in Table 11 was carried out by pumping a continuous slurry (with a known solids concentration) into the column, we were able to independently (a) determine the liquid axial dispersion coefficient in the presence of fine particles at a uniform concentration of solids and (b) compare the effect of varying solids concentration on liquid axial dispersion coefficients. As discussed earlier, unusual behavior was observed in the absence of a distributor plate. The liquid level at the top of the column periodically surged so that the liquid level rose above the exit line and then suddenly drop a few inches below the exit line. Periodic gas slugs were usually observed in the column and were suspected to be the major case of the surging behavior. Because of the surging behavior, the electronic noise in the experimental tracer curve increases at higher gas and liquid velocities reducing data accuracy. For example, Run numbers XX-1 and XX-2 shown in Table 11 were conducted under severe surging conditions. The dispersion coefficients obtained from these two experiments were completely out of line with the rest of data and were excluded in the following discussion.

5.2.2.1 Effect of Liquid Velocity

In general, liquid velocity had no effect on the liquid dispersion coefficient. In the presence of distributor #1, the results for two particle sizes (20/30 and 60/80 mesh) at three concentrations (0, 5, and 20 lb/ft^3) are summarized in Table 12. The data were taken at a constant gas velocity of 0.327 ft/sec., while the liquid velocity ranged from 0.009 to 0.059 ft/sec. Without solids, a fivefold increase of liquid velocity from 0.009 to 0.049 ft/sec. did not change the value of the liquid dispersion coefficient. A similar lack of dependence

Table 12

Effect of Liquid Velocity on Axial Liquid Dispersion Coefficient in the Presence of Distributor #1

Gas Velocity = 0.327 ft/sec

Liquid velocity (ft/sec)	Axial dispersion coefficient (ft^2/sec)				
	No solids	20/30 mesh		60/80 mesh	
		C_S[a] = 5.0 lb/ft^3	C_S = 20.0 lb/ft^3	C_S = 5.0 lb/ft^3	C_S = 20.0 lb/ft^3
0.009	0.61	0.51			
0.013			0.20		
0.018				0.43	0.46
0.026			0.38		
0.030		0.48	0.50	0.38	
0.035				0.44	
0.040		0.47	0.36		0.45
0.049	0.62		0.38	0.42	
0.053		0.47		0.48	
0.059		0.48			

[a] C_S = concentration of solids.

on liquid velocity was observed in the presence of solid particles. At a low solid concentration (5 lb/ft^3), the liquid dispersion coefficient was independent of liquid velocity for both 20/30 and 60/80 mesh particles. However, at high concentrations (20 lb/ft^3), the data for 20/30 mesh particles all scattered, at 0.013 and 0.030 ft/sec liquid velocity. At these conditions, discrepancies were also observed between the predicted and theoretical curves. These discrepancies are not clearly understood. Since the large particles (20/30 mesh) were not completely suspended at these operating conditions, the settled solids at high concentrations could be the cause of the observed discrepancies. In any event, such discrepancies were not observed for high concentrations of 60/80 mesh particles. In general, liquid velocity has no effect on the liquid dispersion coefficient in the presence of distributor #1.

Similarly the results for distributor #2 also show that the liquid dispersion coefficient is independent of liquid velocity (Table 13). Although larger data scattering was observed without solids present, there is no trend that indicates dependence on liquid velocity. Furthermore, the data obtained in the presence of solids clearly indicated that the liquid dispersion coefficient was independent of liquid velocity at all conditions.

Although limited data were available because of the surging behavior in the absence of a distributor plate, the results consistently indicated that liquid velocity did not effect the liquid dispersion coefficient. For example, in the absence of solids, increasing liquid velocity from 0.015 to 0.041 ft/sec resulted in an insignificant change in axial dispersion coefficients (0.475 to 0.513 ft^2/sec). Similarly, increasing liquid velocity from 0.021 to 0.053 ft/sec in the presence of 20/30 mesh and -140 mesh particles resulted in a negligible change in axial dispersion coefficient, from 0.466 to 0.472 and from 0.452 to 0.404 ft^2/sec, respectively. All these results show consistently that liquid velocity has no effect on axial dispersion coefficients.

Table 13

Effect of Liquid Velocity on Axial
Dispersion Coefficients in the Presence of Distributor #2

Gas Velocity = 0.327 ft/sec

	Axial dispersion coefficients (ft^2/sec)				
V_L		20/30 mesh		-140 mesh	
(ft/sec)	No solids	C_s = 5 lb/ft^3	C_s = 20 lbs/ft^3	C_s = 3.7 lb/ft^3	C_s = 14.9 lb/ft^3
0.02	0.54	0.43	0.37	0.45	0.34
0.04	0.61	0.43	0.32	0.42	0.36
0.05	0.48	0.40	0.36	0.41	0.40